Supplementary Information

Multichrome encoding-based multiplexed, spatially resolved imaging reveals single-cell RNA epigenetic modifications heterogeneity

Dongsheng Mao,[1,#] Xiaochen Tang,[2,#] Runchi Zhang,[1] Song Hu,[3] Hongquan Gou,[1] Penghui Zhang,[3] Wenxing Li,[1,*] Qiuhui Pan,[2,*] Bing Shen,[1,*] Xiaoli Zhu[1,*]

[1] Shanghai Tenth People's Hospital of Tongji University, Shanghai 200072, P. R. China.

[2] Department of Clinical Laboratory Medicine, Shanghai Children's Medical Center, Shanghai Jiao Tong University School of Medicine, Shanghai 200127, P. R. China.

[3] Shanghai Pudong New Area People's Hospital, Shanghai 201299, P. R. China.

[#] These authors contributed equally to this work.

[*]Corresponding authors:

Wenxing Li, Email: wenxingapp@163.com

Qiuhui Pan, Email: panqiuhui_med@163.com

Bing Shen, Email: urodrshenbing@shsmu.edu.cn

Xiaoli Zhu, Email: xiaolizhu@tongji.edu.cn

Supplementary figures

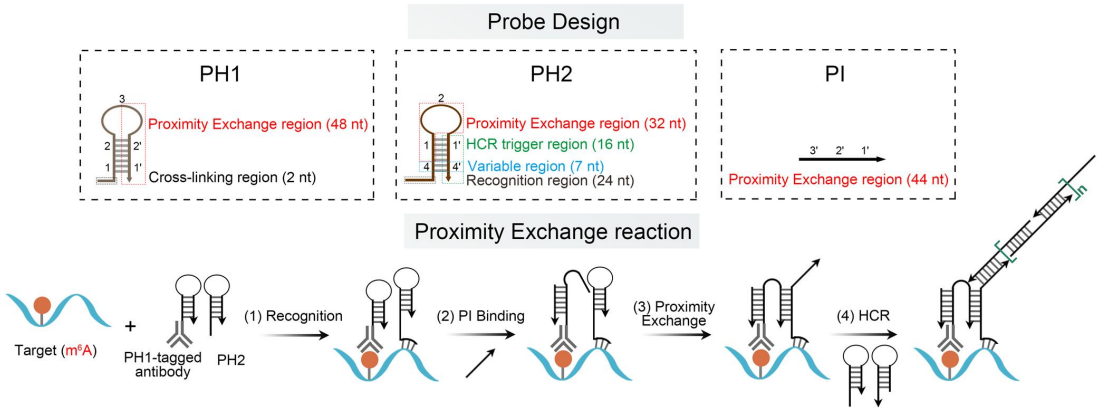

Supplementary Fig. 1 | Schematic illustration of the structure and workflow of each element in PREEM. Top, schematic diagram of probe design in three PREEM elements. Bottom, schematic diagram of proximity exchange reaction.

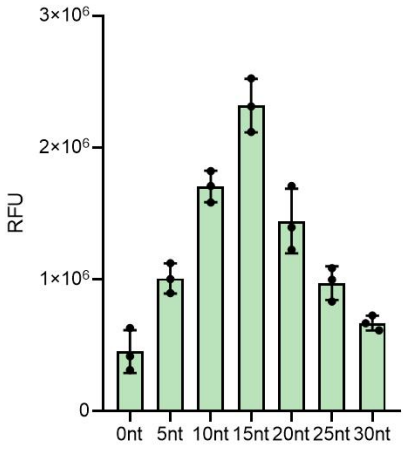

Supplementary Fig. 2 | The impact of the distance between PH2 and the m^{6}A site on proximity exchange reaction from 3 independent experiments. Data are presented as mean values ± s.d. Source data are provided as a Source Data file.

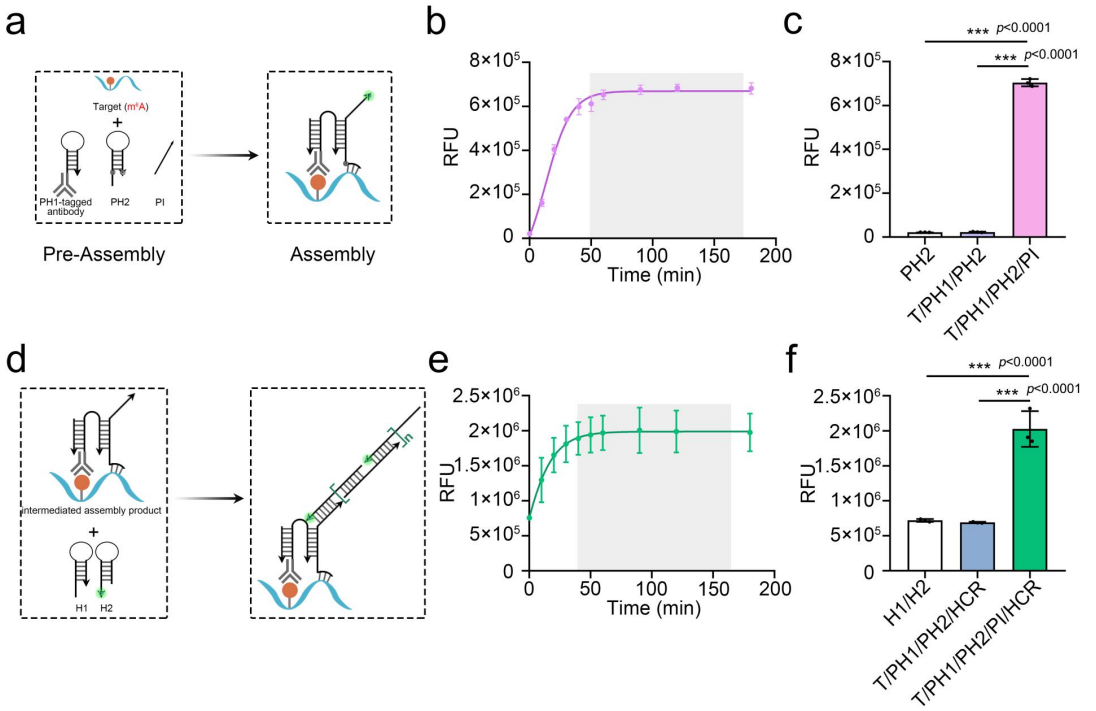

Supplementary Fig. 3 | Proximity exchange reaction-mediated m^{6}A RNA analysis. a) Schematic illustration of proximity exchange reaction. b) Kinetic curve of PI hybridization on different times (from 0 to 180 min) from 3 independent experiments. c) Quantification of different groups in the proximity exchange reaction from 3 independent experiments. d) Schematic illustration of proximity exchange-assisted HCR. e) Kinetic curve of HCR on different times (from 0 to 180 min) from 3 independent experiments. f) Quantification of different groups in the HCR from 3 independent experiments. * $p < 0.05$, ** $p < 0.01$, *** $p < 0.001$. Data are presented as mean values ± s.d. Error bars represent the standard deviation of three independent experiments. Source data are provided as a Source Data file.

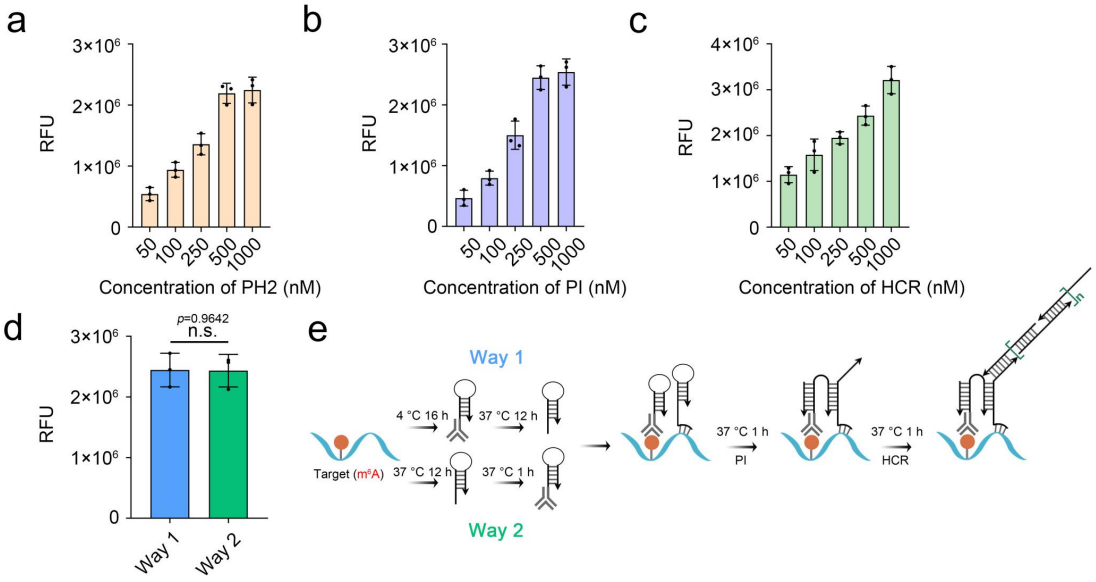

Supplementary Fig. 4 | Optimization of the concentration of each component and reaction time in PREEM system. a) Optimization of the concentration of PH2 probe in the proximity exchange reaction from 3 independent experiments.. b) Optimization of the concentration of PI probe in the proximity exchange reaction from 3 independent experiments. c) Optimization of the concentration of HCR probes in the proximity exchange reaction from 3 independent experiments. d) Comparison of the performance of different experiment processes in the proximity exchange reaction from 3 independent experiments. Way 1, incubating the antibody at 4 °C overnight (16 h) and then hybridizing the probes at 37 °C for 12 h; Way 2, hybridizing the probes at 37 °C overnight for 12 h and incubating the antibody at 37 °C 1 h. *n.s.*, no significance. e) Schematic illustration of different experiment processes in the proximity exchange reaction. Data are presented as mean values ± s.d. Error bars represent the standard deviation of three independent experiments. Source data are provided as a Source Data file.

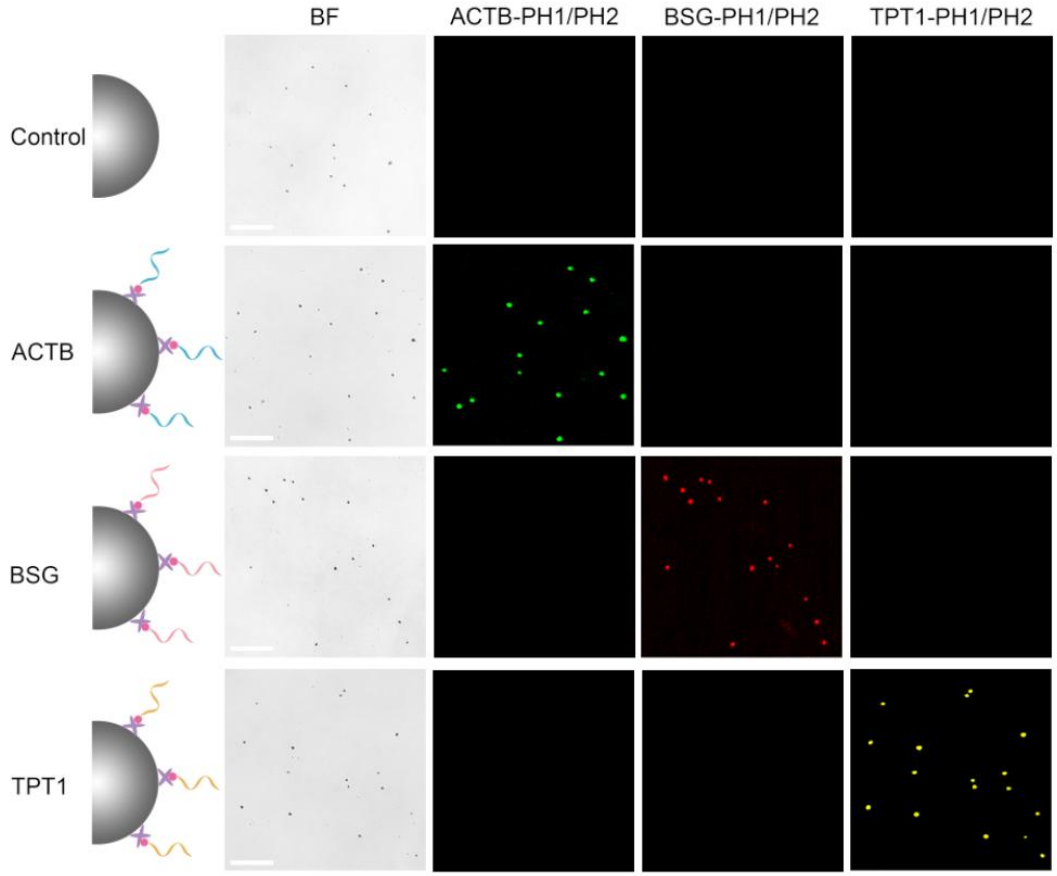

Supplementary Fig. 5 | The orthogonal reactivity of PREEM characterized in MMB-based PREEM for the simulation detection of m^{6}A RNA from 3 independent experiments. Scale bars: 10 μm.

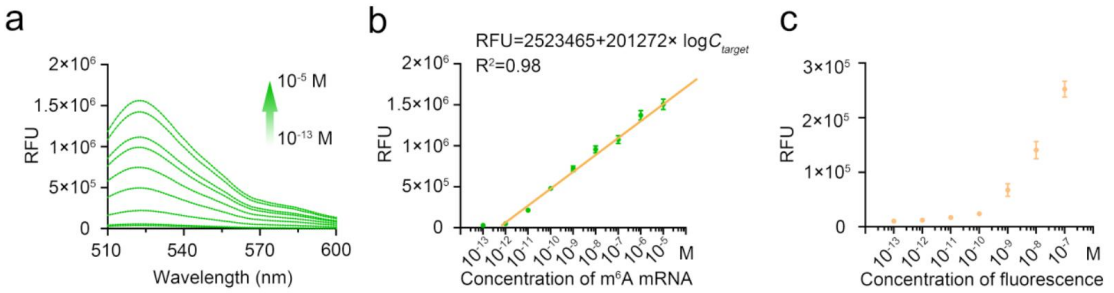

Supplementary Fig. 6 | Study of the detection sensitivity of PREEM in the test tube. a) Fluorescence spectrum of targets in different concentrations by PREEM system from 3 independent experiments. b) Correlation analysis between different concentration groups from 3 independent experiments. The yellow line indicates the relationship between the m^{6}A RNA concentration and the average fluorescence of each group (R^2 = 0.98). c) Detection limit of fluorescence concentration (buffer with fluorescent nucleic acids) analyzed by using the same instrument from 3 independent experiments. Data are presented as mean values ± s.d. Error bars represent the standard deviation of three independent experiments. Source data are provided as a Source Data file.

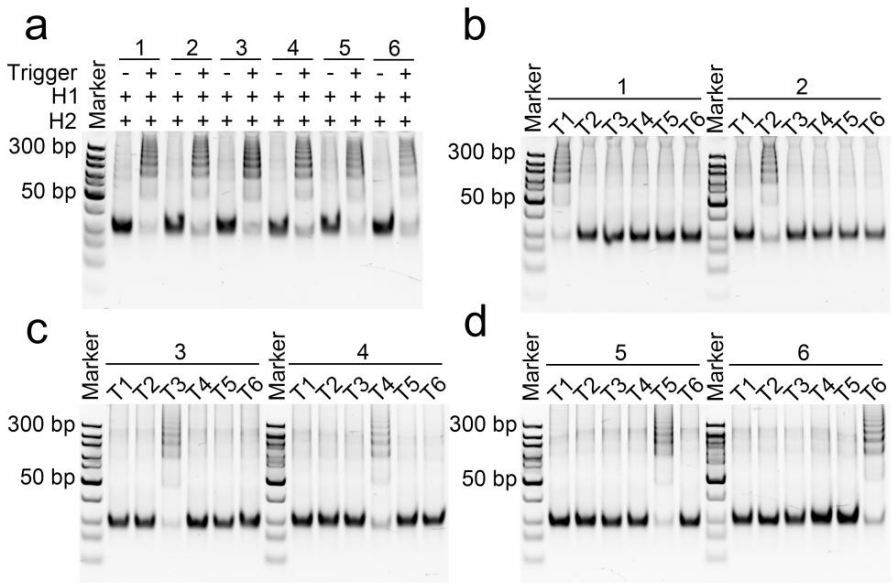

Supplementary Fig. 7 | Feasibility and orthogonality of HCR. PAGE analysis of the assembly (a) and orthogonality (b-d) of six groups of HCR. Source data are provided as a Source Data file.

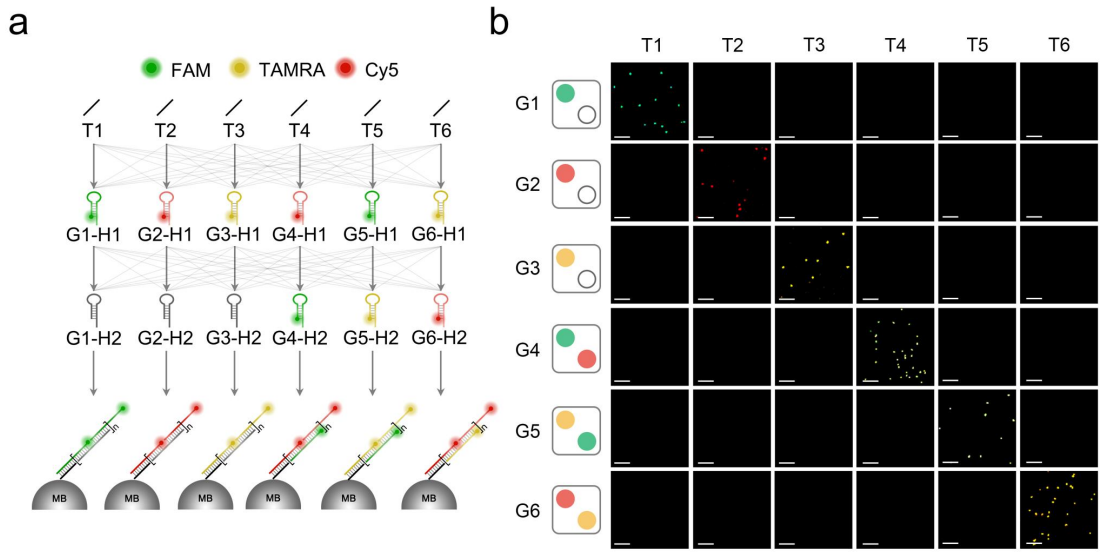

Supplementary Fig. 8 | The orthogonal reactivity of PREEM characterized on MMB model from 3 independent experiments. Scale bars: 10 μm.

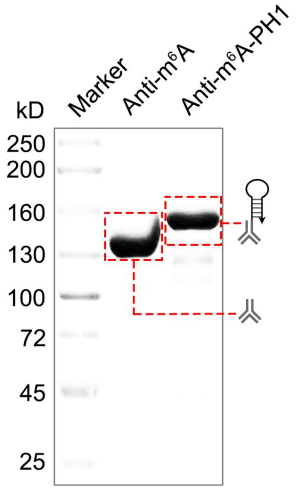

Supplementary Fig. 9 | Non-reducing SDS-PAGE image of coomassie blue stained anti-m^{6}A-PH1 conjugate. Source data are provided as a Source Data file.

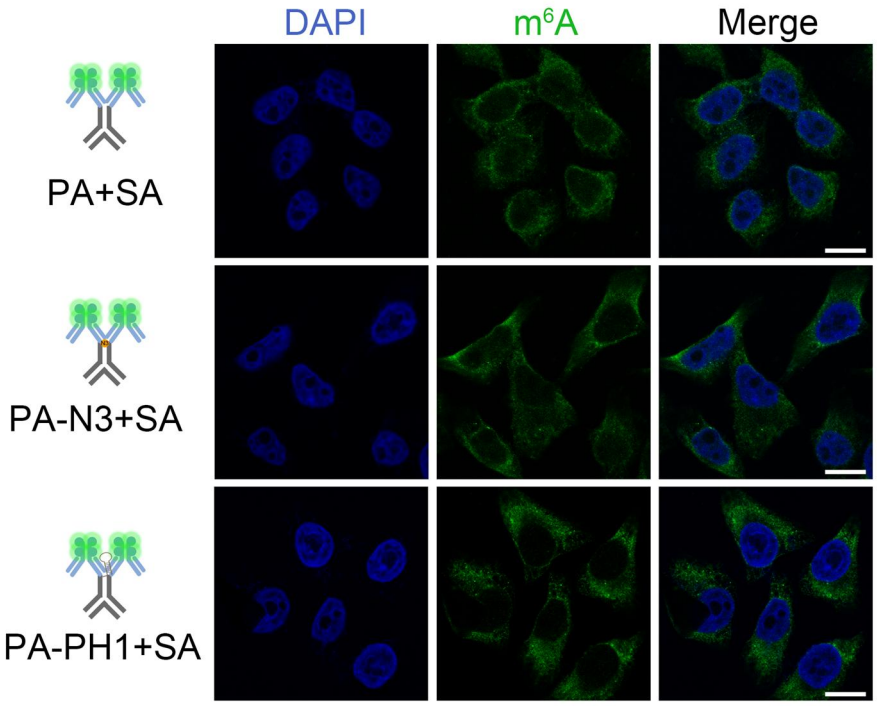

Supplementary Fig. 10 | Conventional immunofluorescence (IF) of m^{6}A modification on HeLa cells from 3 independent experiments. The primary antibody (PA) was either used as-unmodified, or modified with the crosslinker (NHS-PEG$_4$-Azide), or labeled with PH1. Alexa Fluor® 488-modified secondary antibody (SA) was adopted for imaging. Scale bars: 10 μm.

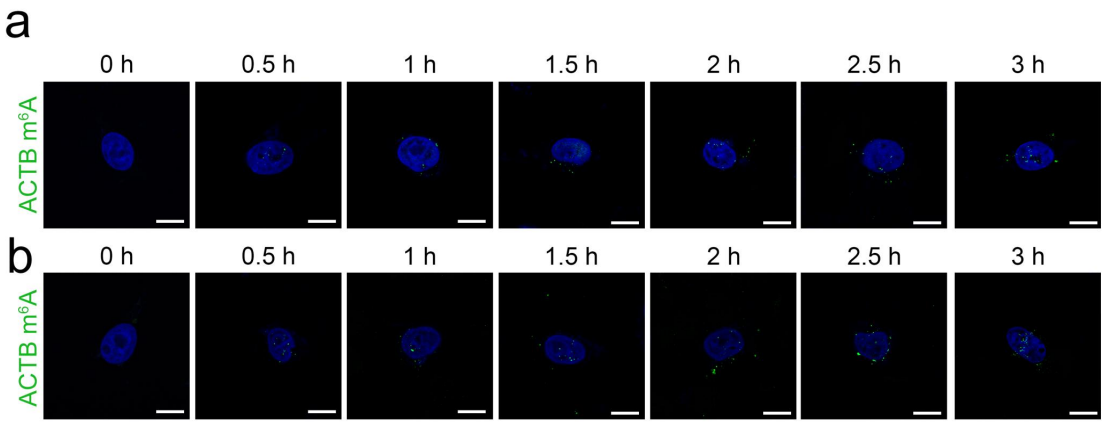

Supplementary Fig. 11 | Optimization of reaction conditions. Optimization of the reaction time including PI hybridization (a) and HCR (b) in HeLa cells from 3 independent experiments. Scale bars: 10 μm.

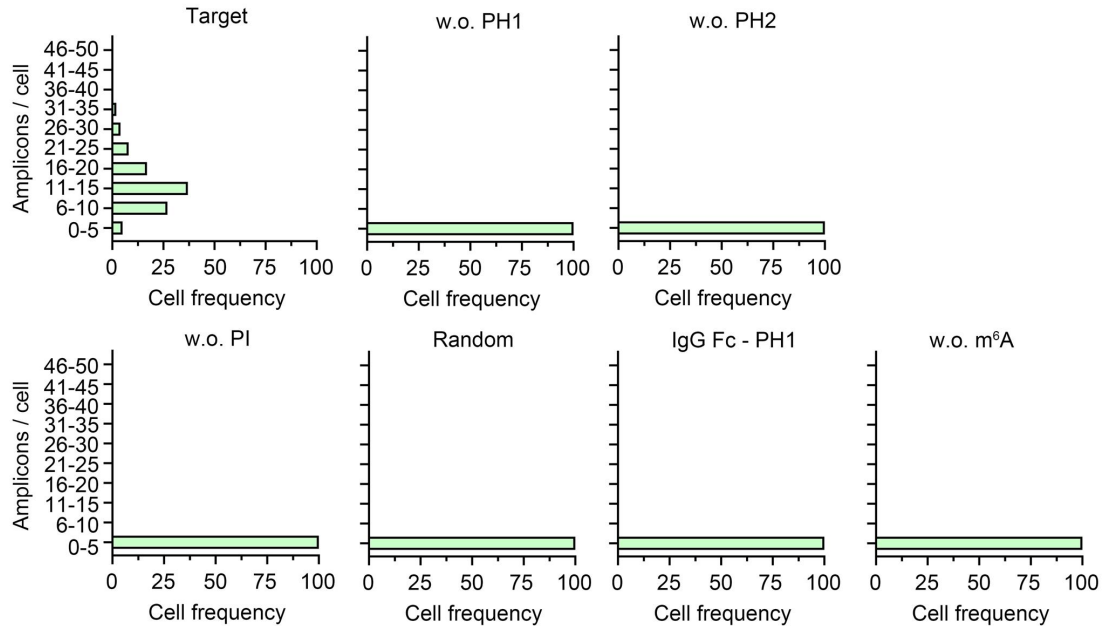

Supplementary Fig. 12 | Frequency histograms of amplicons counted for different groups in single cells (*N* = 100). *N* represents the number of single cells for each sample. Source data are provided as a Source Data file.

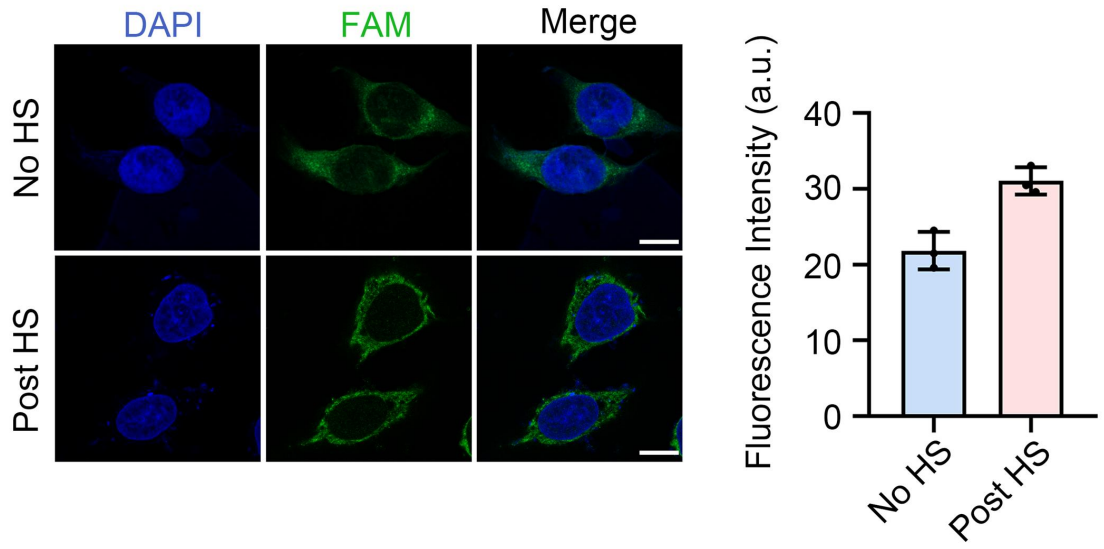

Supplementary Fig. 13 | Fluorescence images of m^{6}A level visualized by IF in HeLa cells with or without heat shock treatment from 3 independent experiments. Scale bars: 10 μm. Right, quantitative bar plots analyzed by ImageJ software of the fluorescence intensity of the images shown in left. Data are presented as mean values ± s.d. Error bars represent the standard deviation of three independent experiments. Source data are provided as a Source Data file.

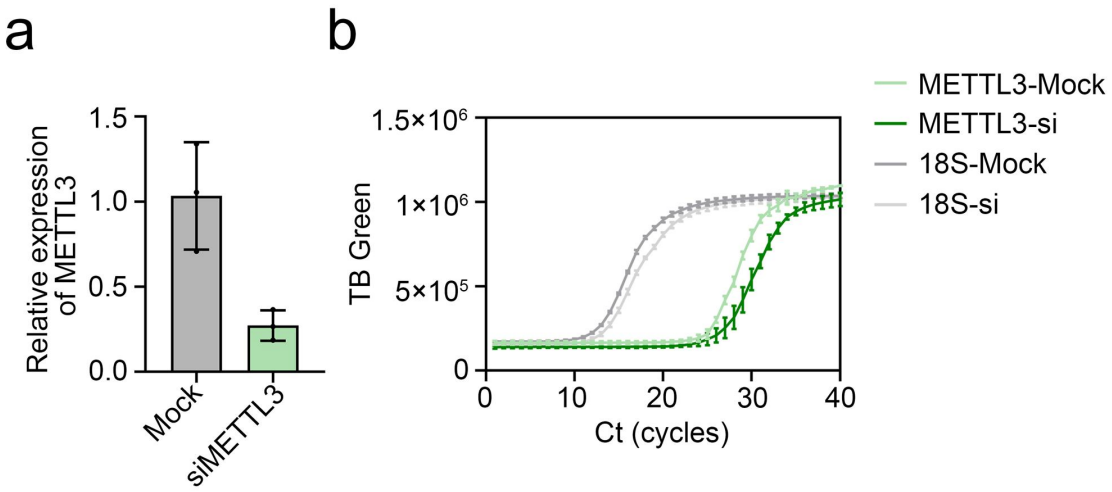

Supplementary Fig. 14 | Expression analysis of 18S and METTL3 mRNA in HeLa cells by RT-qPCR. a) Relative expression level of METTL3 before (Mock) and after knockdown (siMETTL3) from 3 independent experiments. b) Real-time fluorescence curves in RT-qPCR analysis from 3 independent experiments. Data are presented as mean values ± s.d. Error bars represent the standard deviation of three independent experiments. Source data are provided as a Source Data file.

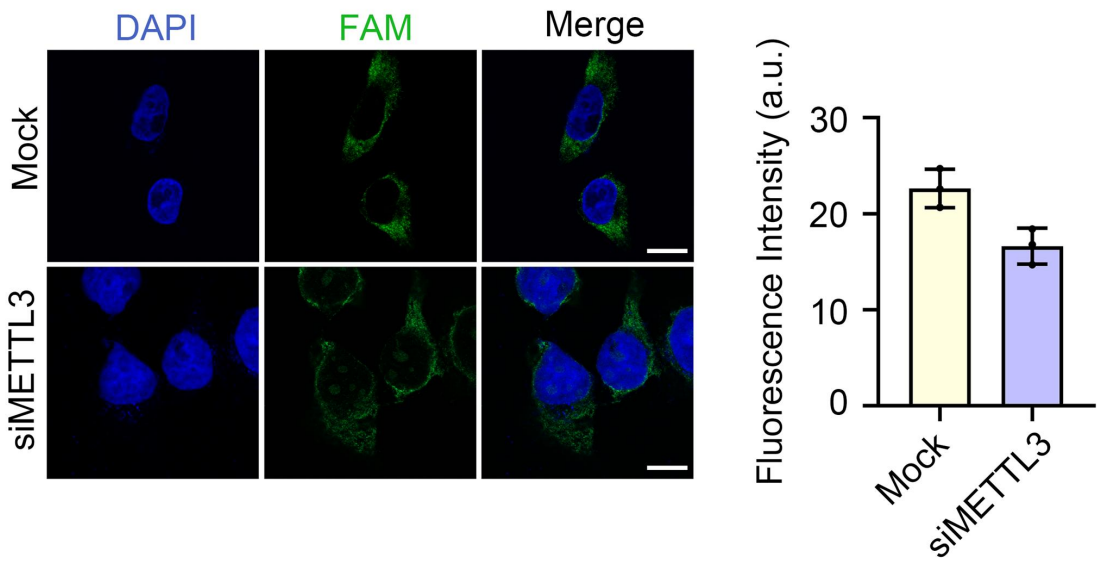

Supplementary Fig. 15 | Fluorescence images of m^{6}A level visualized by IF in HeLa cells upon METTL3 knockdown from 3 independent experiments. Scale bars: 10 μm. Right, quantitative bar plots analyzed by ImageJ software of the fluorescence intensity of the images shown in left. Data are presented as mean values ± s.d. Error bars represent the standard deviation of three independent experiments. Source data are provided as a Source Data file.

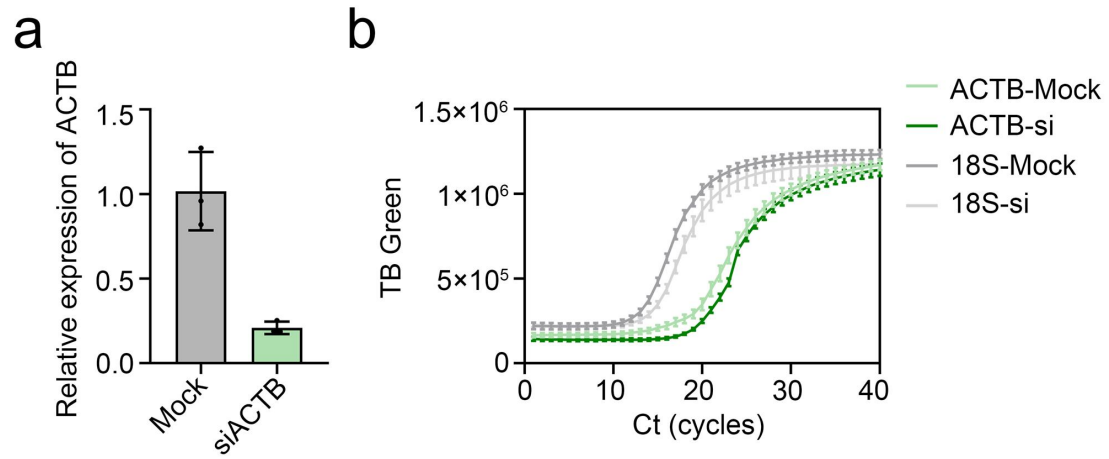

Supplementary Fig. 16 | Expression analysis of 18S and ACTB mRNA in HeLa cells by RT-qPCR. a) Relative expression level of ACTB before (Mock) and after knockdown (siACTB) from 3 independent experiments. b) Real-time fluorescence curves in RT-qPCR analysis from 3 independent experiments. Data are presented as mean values ± s.d. Error bars represent the standard deviation of three independent experiments. Source data are provided as a Source Data file.

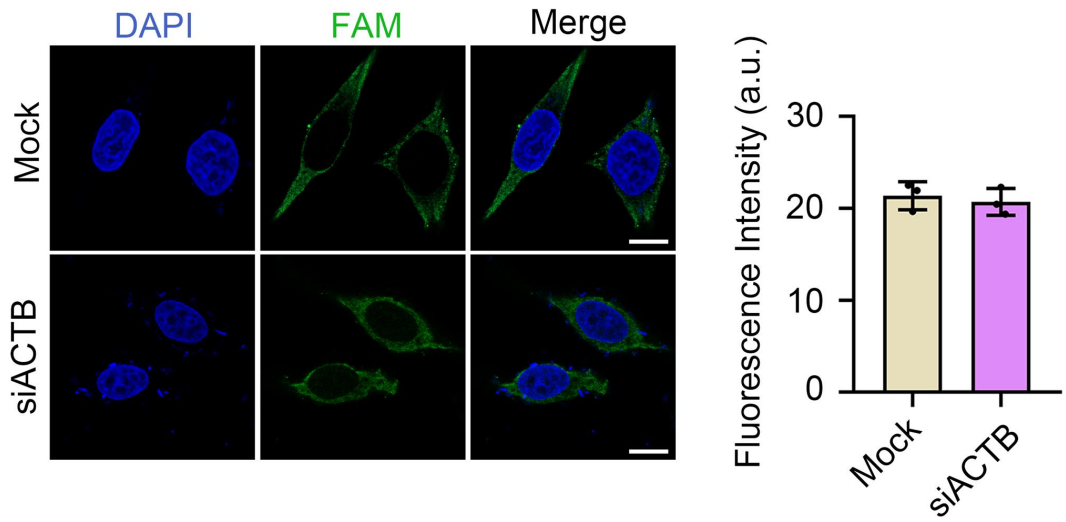

Supplementary Fig. 17 | Fluorescence images of m^{6}A level visualized by IF in HeLa cells upon ACTB knockdown from 3 independent experiments. Scale bars: 10 μm. Right, quantitative bar plots analyzed by ImageJ software of the fluorescence intensity of the images shown in left. Data are presented as mean values ± s.d. Error bars represent the standard deviation of three independent experiments. Source data are provided as a Source Data file.

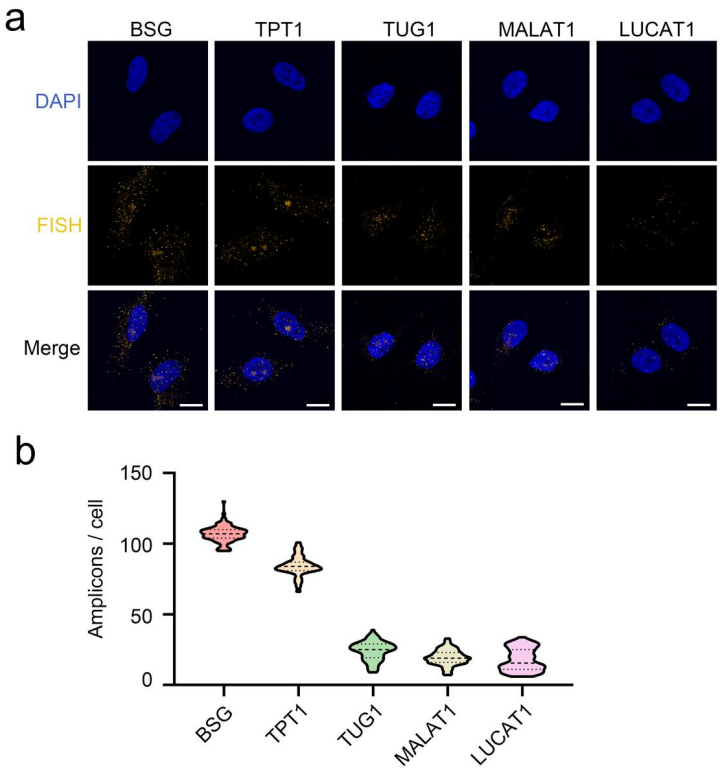

Supplementary Fig. 18 | Quantitative analysis of RNAs based on FISH. a) Fluorescence imaging of BSG, TPT1, TUG1, MALAT1, and LUCAT1 RNA by FISH in single cells. Scale bars: 10 μm. b) Violin chart of amplicons counted for each sample in single cells (N = 100). N represents the number of single cells for each sample. Source data are provided as a Source Data file.

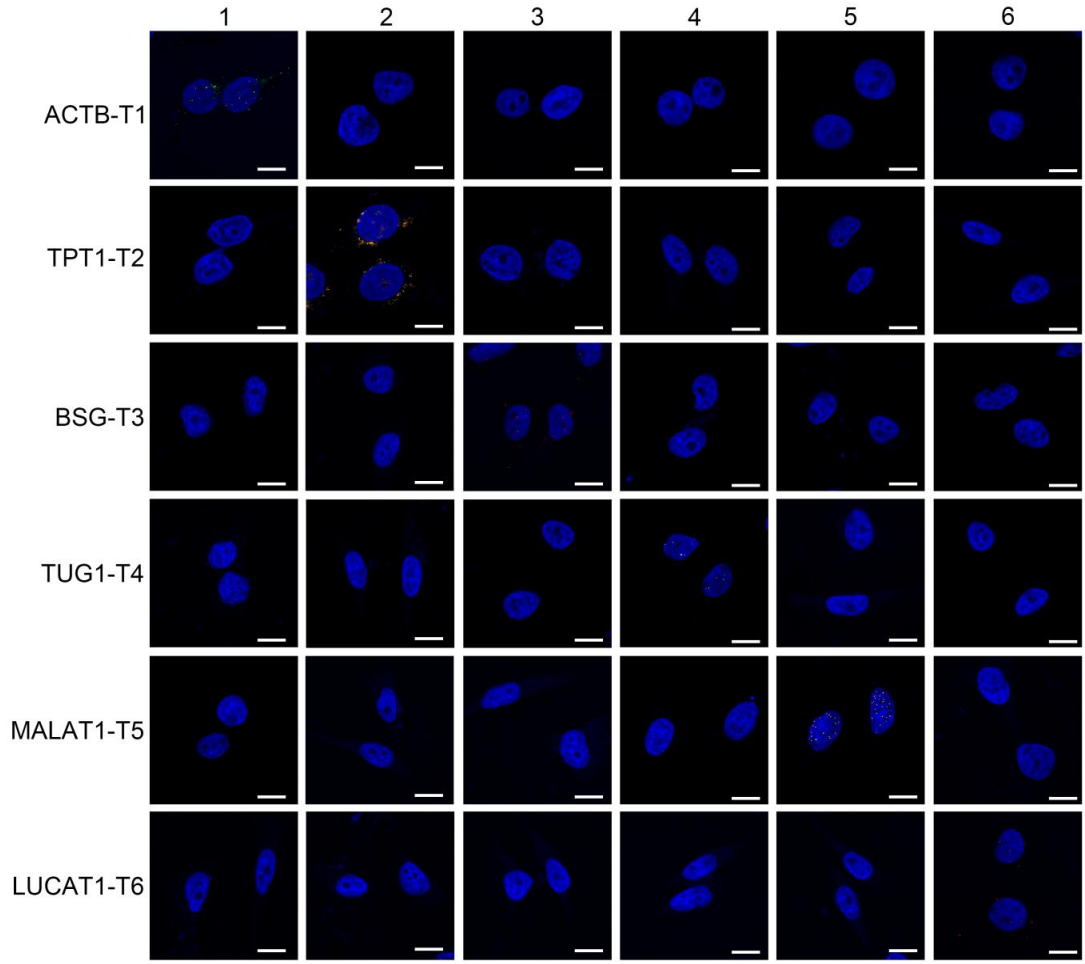

Supplementary Fig. 19 | Orthogonal imaging of six m^{6}A RNAs in HeLa cells by PREEM from 3 independent experiments. Scale bars: 10 μm.

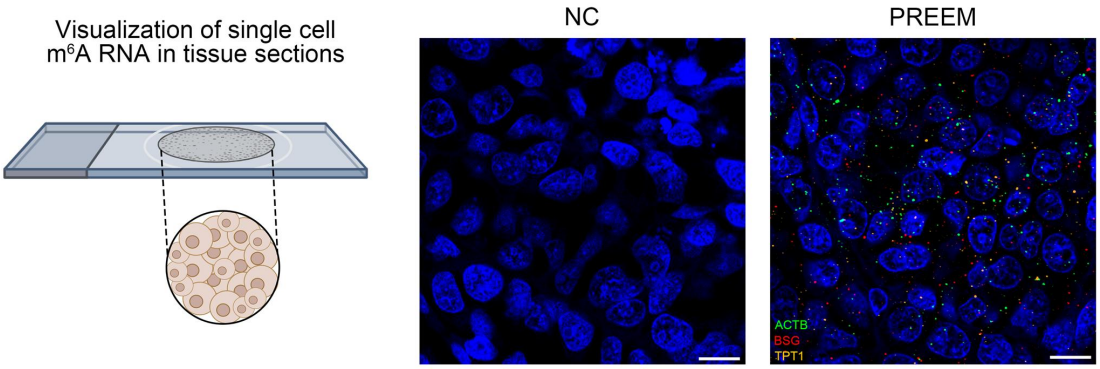

Supplementary Fig. 20 | Profiling of m^{6}A RNAs in mouse liver tissues by PREEM from 3 independent experiments. NC, incubated with HCR. Scale bars: 10 μm.

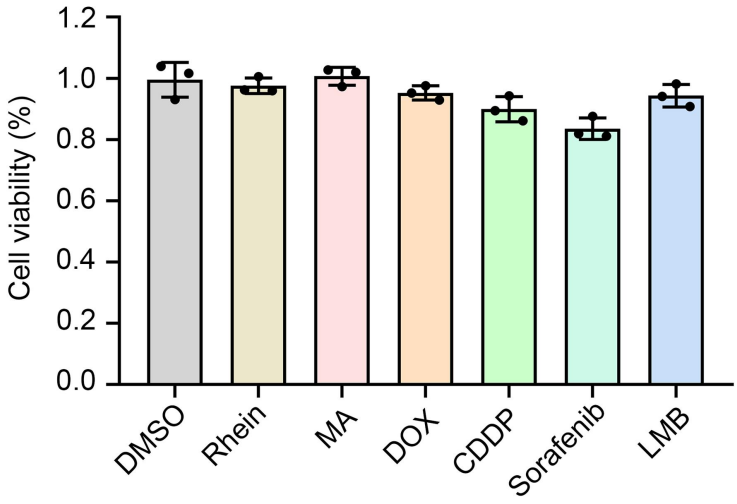

Supplementary Fig. 21 | Cell viability quantification of CCK-8 assay with different drugs treated from 3 independent experiments. Data are presented as mean values ± s.d. Error bars represent the standard deviation of three independent experiments. Source data are provided as a Source Data file.

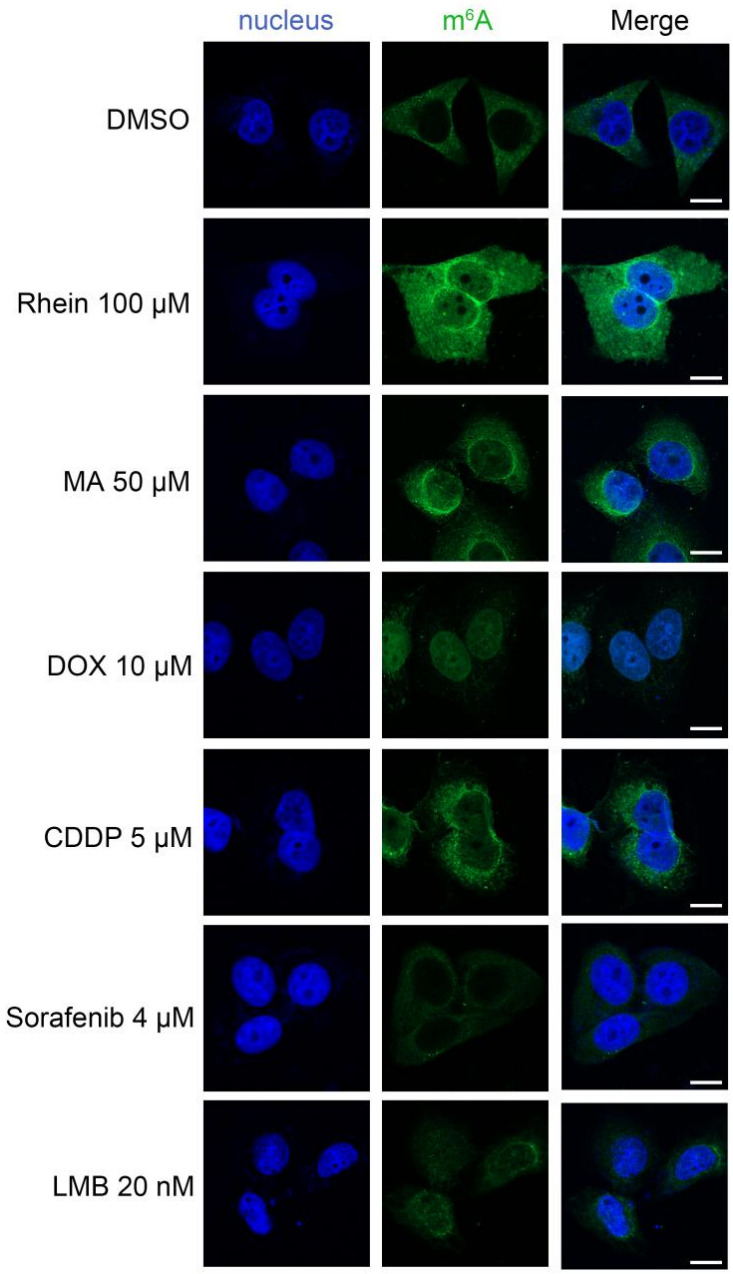

Supplementary Fig. 22 | Fluorescence images of m^{6}A level visualized by IF in HeLa cells with different drugs treated from 3 independent experiments. Scale bars: 10 μm.

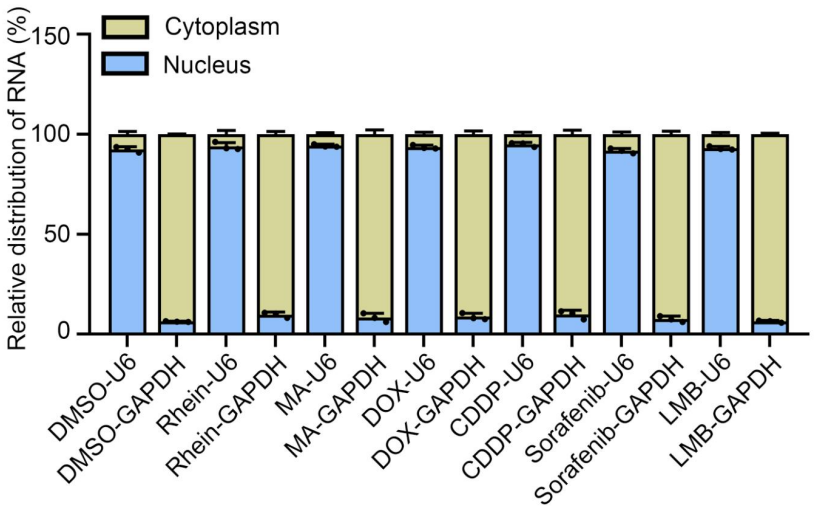

Supplementary Fig. 23 | Comparison of nuclear (U6) and cytoplasmic (GAPDH) marker enrichment detected by RT-qPCR between fractions from DMSO (NC) and drug treated groups from 3 independent experiments. Data are presented as mean values ± s.d. Error bars represent the standard deviation of three independent experiments. Source data are provided as a Source Data file.

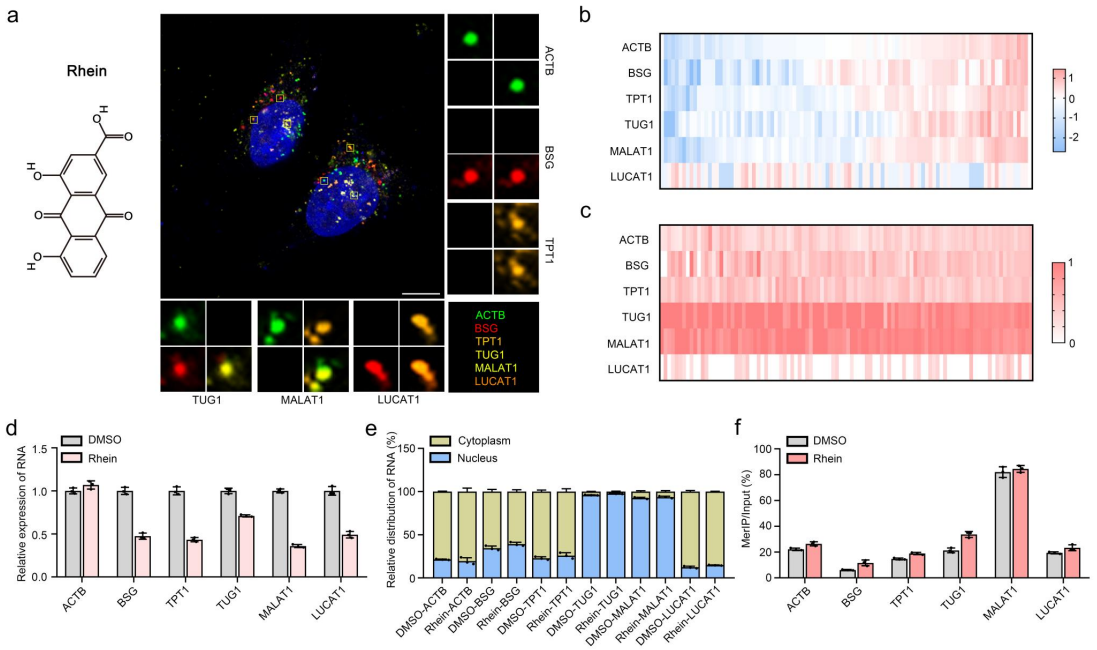

Supplementary Fig. 24 | Profiling of m^{6}A RNAs in HeLa cells with Rhein treated. a) Fluorescence images of six RNA-m^{6}A level visualized by PREEM in HeLa cells with Rhein treated. Scale bars: 10 μm. b) Heat map showing expression pattern of six m^{6}A RNAs with Rhein treated by analyzing the amplicons in cells by PREEM. c) Heat map showing subcellular distribution of six m^{6}A RNAs with Rhein treated. d) Expression analysis of six RNAs in HeLa cells with Rhein treated quantified by RT-qPCR. e) Six RNAs show relative distribution in HeLa cells with Rhein treated quantified by qRT-PCR. f) m^{6}A-IP combined with RT-qPCR to quantify the relative m^{6}A level of six RNAs in HeLa cells with Rhein treated. Data are presented as mean values ± s.d. Error bars represent the standard deviation of three independent experiments. Source data are provided as a Source Data file.

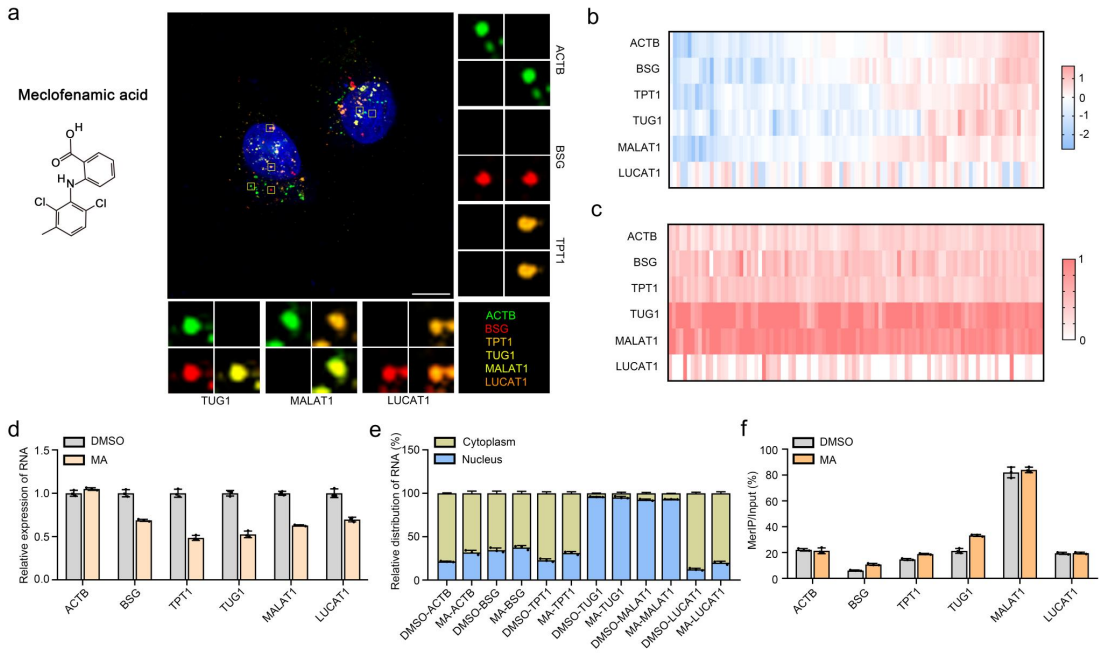

Supplementary Fig. 25 | Profiling of m^{6}A RNAs in HeLa cells with meclofenamic acid (MA) treated. a) Fluorescence images of six RNA-m^{6}A level visualized by PREEM in HeLa cells with MA treated. Scale bars: 10 μm. b) Heat map showing expression pattern of six m^{6}A RNAs with MA treated by analyzing the amplicons in cells by PREEM. c) Heat map showing subcellular distribution of six m^{6}A RNAs with MA treated. d) Expression analysis of six RNAs in HeLa cells with MA treated quantified by RT-qPCR. e) Six RNAs show relative distribution in HeLa cells with MA treated quantified by qRT-PCR. f) m^{6}A-IP combined with RT-qPCR to quantify the relative m^{6}A level of six RNAs in HeLa cells with MA treated. Data are presented as mean values ± s.d. Error bars represent the standard deviation of three independent experiments. Source data are provided as a Source Data file.

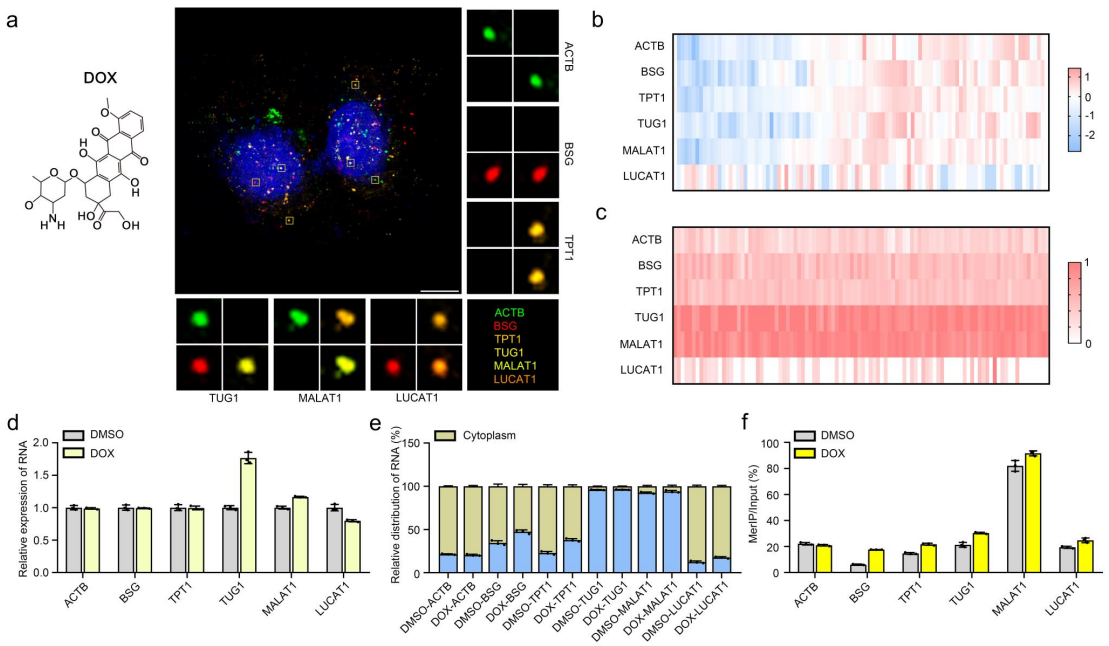

Supplementary Fig. 26 | Profiling of m^{6}A RNAs in HeLa cells with DOX treated. a) Fluorescence images of six RNA-m^{6}A level visualized by PREEM in HeLa cells with DOX treated. Scale bars: 10 μm. b) Heat map showing expression pattern of six m^{6}A RNAs with DOX treated by analyzing the amplicons in cells by PREEM. c) Heat map showing subcellular distribution of six m^{6}A RNAs with DOX treated. d) Expression analysis of six RNAs in HeLa cells with DOX treated quantified by RT-qPCR. e) Six RNAs show relative distribution in HeLa cells with DOX treated quantified by qRT-PCR. f) m^{6}A-IP combined with RT-qPCR to quantify the relative m^{6}A level of six RNAs in HeLa cells with DOX treated. Data are presented as mean values ± s.d. Error bars represent the standard deviation of three independent experiments. Source data are provided as a Source Data file.

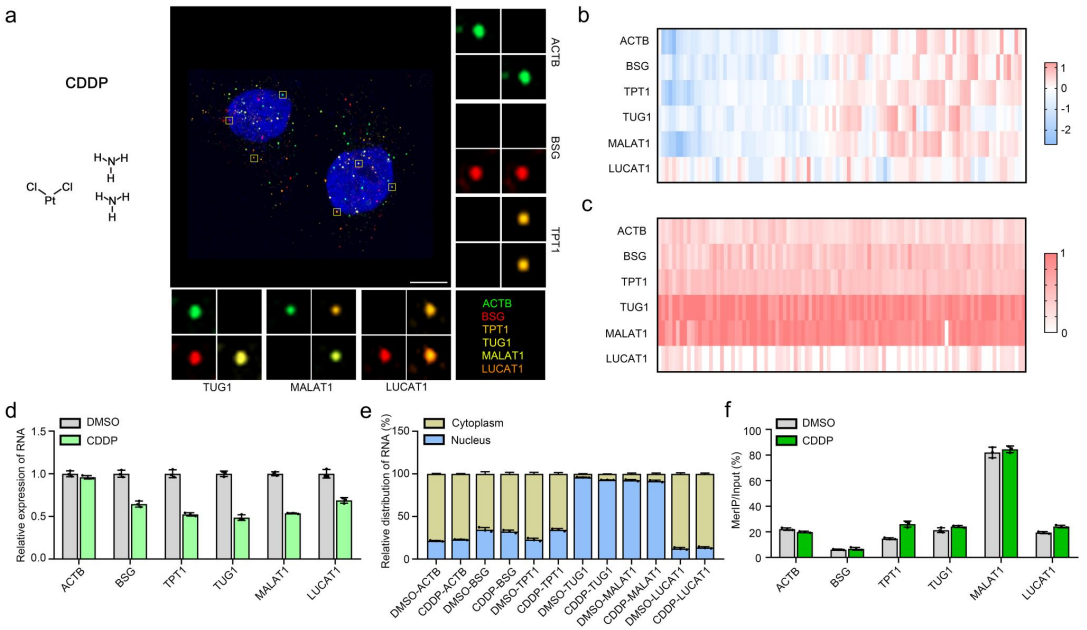

Supplementary Fig. 27 | Profiling of m^{6}A RNAs in HeLa cells with CDDP treated. a) Fluorescence images of six RNA-m^{6}A level visualized by PREEM in HeLa cells with CDDP treated. Scale bars: 10 μm. b) Heat map showing expression pattern of six m^{6}A RNAs with CDDP treated by analyzing the amplicons in cells by PREEM. c) Heat map showing subcellular distribution of six m^{6}A RNAs with CDDP treated. d) Expression analysis of six RNAs in HeLa cells with CDDP treated quantified by RT-qPCR. e) Six RNAs show relative distribution in HeLa cells with CDDP treated quantified by qRT-PCR. f) m^{6}A-IP combined with RT-qPCR to quantify the relative m^{6}A level of six RNAs in HeLa cells with CDDP treated. Data are presented as mean values ± s.d. Error bars represent the standard deviation of three independent experiments. Source data are provided as a Source Data file.

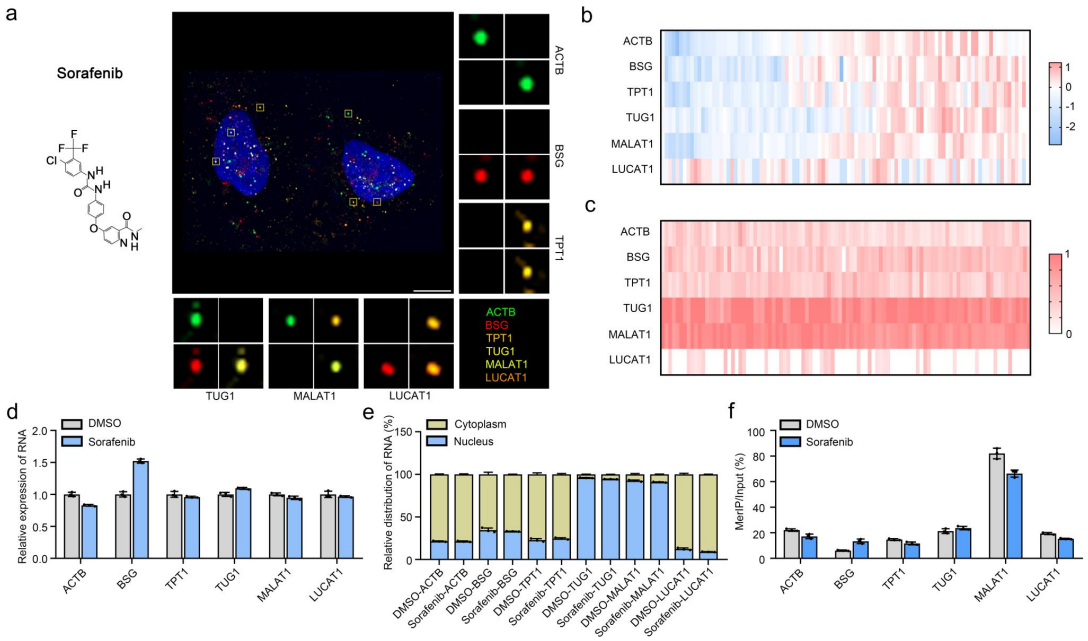

Supplementary Fig. 28 | Profiling of m^{6}A RNAs in HeLa cells with Sorafenib treated. a) Fluorescence images of six RNA-m^{6}A level visualized by PREEM in HeLa cells with Sorafenib treated. Scale bars: 10 μm. b) Heat map showing expression pattern of six m^{6}A RNAs with Sorafenib treated by analyzing the amplicons in cells by PREEM. c) Heat map showing subcellular distribution of six m^{6}A RNAs with Sorafenib treated. d) Expression analysis of six RNAs in HeLa cells with Sorafenib treated quantified by RT-qPCR. e) Six RNAs show relative distribution in HeLa cells with Sorafenib treated quantified by qRT-PCR. f) m^{6}A-IP combined with RT-qPCR to quantify the relative m^{6}A level of six RNAs in HeLa cells with Sorafenib treated. Data are presented as mean values ± s.d. Error bars represent the standard deviation of three independent experiments. Source data are provided as a Source Data file.

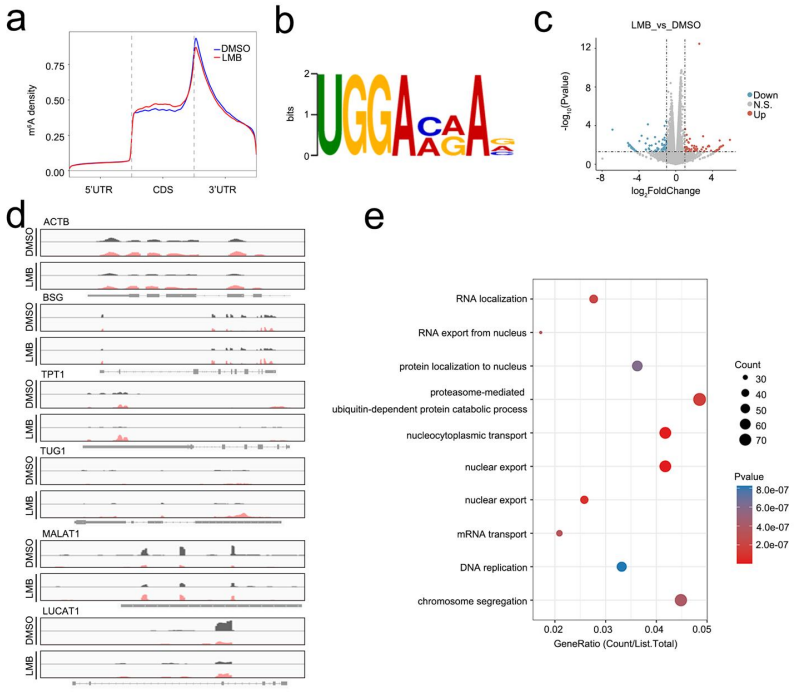

Supplementary Fig. 29 | m^{6}A-Seq profiling of HeLa cells with LMB treated. a) The normalized distribution of m^{6}A peaks across the start codon, CDS, stop codon of RNAs for DMSO and LMB treated m^{6}A peaks. b) Sequence logo representing the consensus motif relative to m^{6}A in response to LMB. c) Volcanic diagram of differentially expressed genes in cells upon LMB treatment. d) Examples of LMB-regulated m^{6}A peaks. In an Integrative Genomics Viewer (IGV) format, normalized m^{6}A-IP and input control coverage are shown in red and gray, respectively. Exons are represented by thick black boxes; 5′ and 3′ untranslated regions (UTRs) are represented by thin black boxes; introns are represented by thin lines. e) GO analysis of transcripts with differentially expressed genes in cells upon LMB treatment.

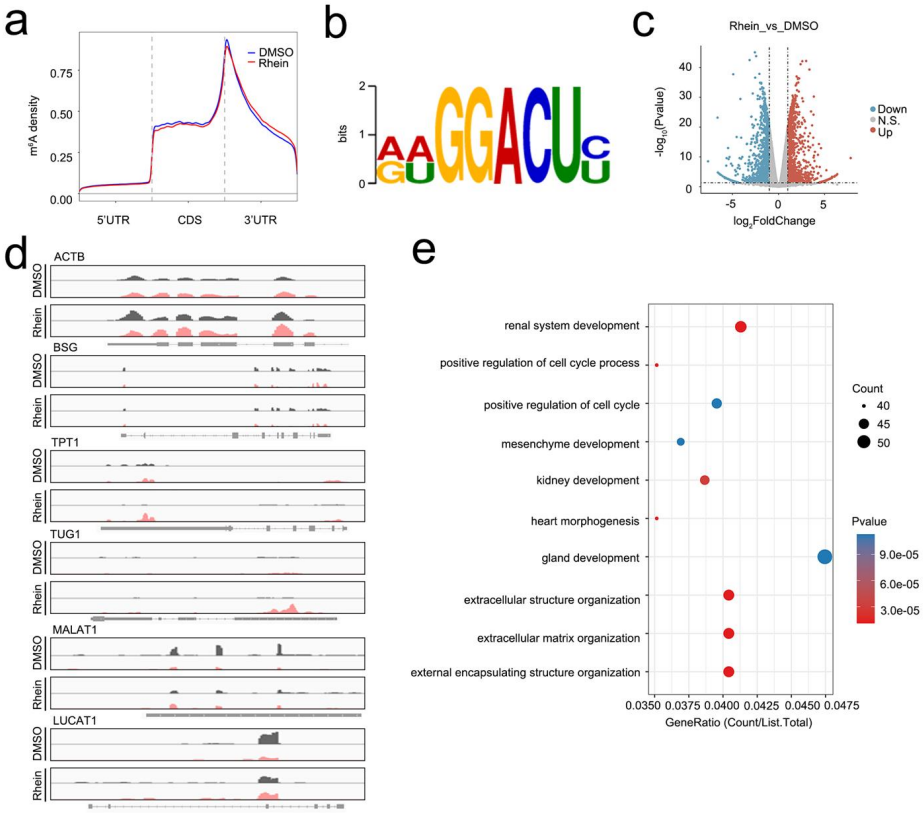

Supplementary Fig. 30 | m^{6}A-Seq profiling of HeLa cells with Rhein treated. a) The normalized distribution of m^{6}A peaks across the start codon, CDS, stop codon of RNAs for DMSO and Rhein treated m^{6}A peaks. b) Sequence logo representing the consensus motif relative to m^{6}A in response to Rhein. c) Volcanic diagram of differentially expressed genes in cells upon Rhein treatment. d) Examples of Rhein-regulated m^{6}A peaks. In an Integrative Genomics Viewer (IGV) format, normalized m^{6}A-IP and input control coverage are shown in red and gray, respectively. Exons are represented by thick black boxes; 5′ and 3′ untranslated regions (UTRs) are represented by thin black boxes; introns are represented by thin lines. e) GO analysis of transcripts with differentially expressed genes in cells upon Rhein treatment.

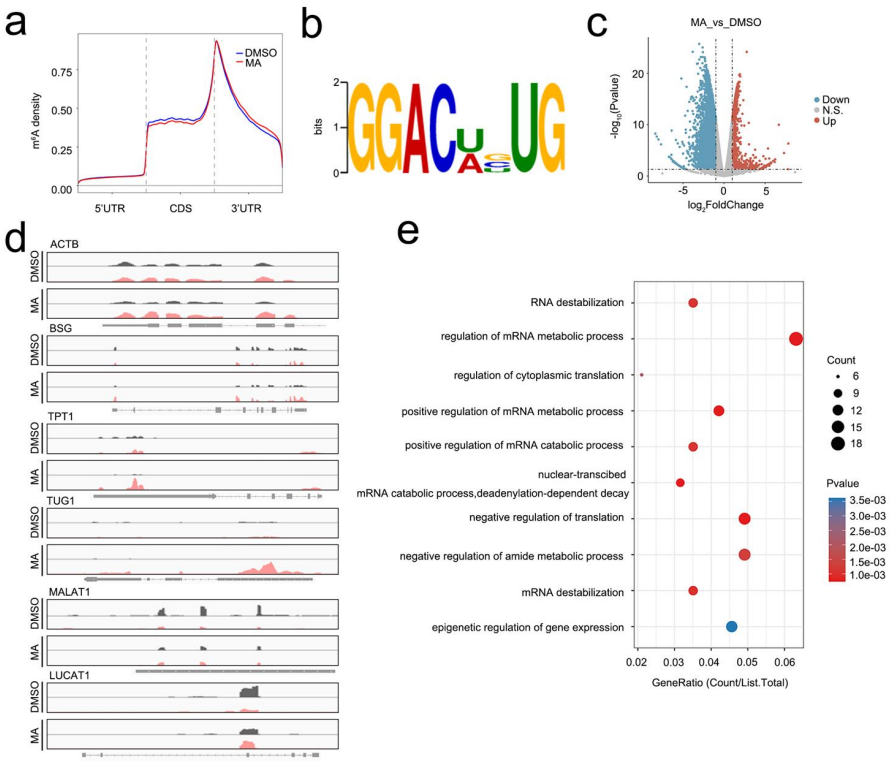

Supplementary Fig. 31 | m^{6}A-Seq profiling of HeLa cells with MA treated. a) The normalized distribution of m^{6}A peaks across the start codon, CDS, stop codon of RNAs for DMSO and MA treated m^{6}A peaks. b) Sequence logo representing the consensus motif relative to m^{6}A in response to MA. c) Volcanic diagram of differentially expressed genes in cells upon MA treatment. d) Examples of MA-regulated m^{6}A peaks. In an Integrative Genomics Viewer (IGV) format, normalized m^{6}A-IP and input control coverage are shown in red and gray, respectively. Exons are represented by thick black boxes; 5′ and 3′ untranslated regions (UTRs) are represented by thin black boxes; introns are represented by thin lines. e) GO analysis of transcripts with differentially expressed genes in cells upon MA treatment.

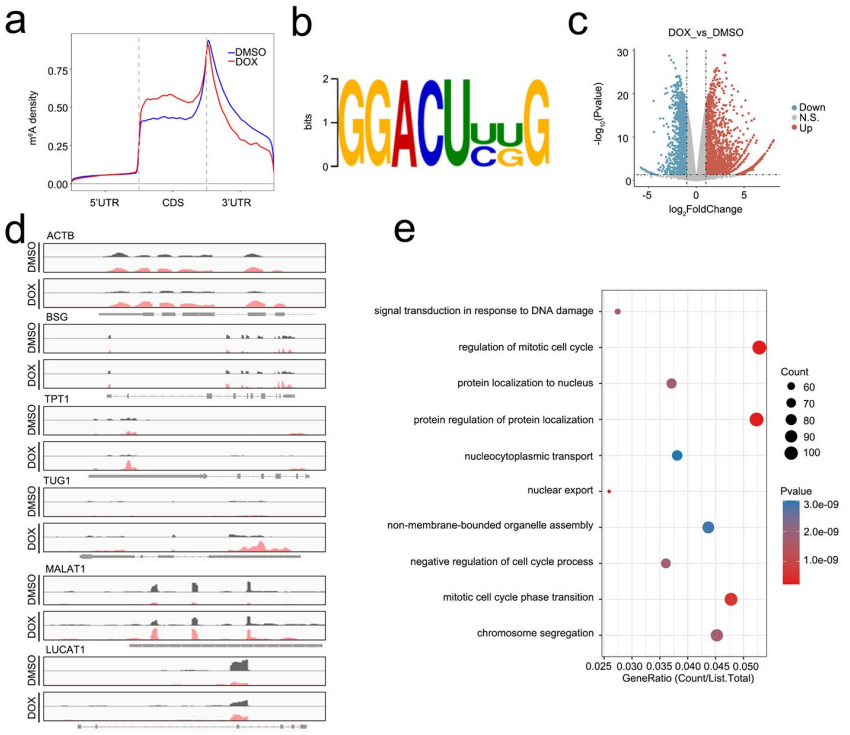

Supplementary Fig. 32 | m^{6}A-Seq profiling of HeLa cells with DOX treated. a) The normalized distribution of m^{6}A peaks across the start codon, CDS, stop codon of RNAs for DMSO and DOX treated m^{6}A peaks. b) Sequence logo representing the consensus motif relative to m^{6}A in response to DOX. c) Volcanic diagram of differentially expressed genes in cells upon DOX treatment. d) Examples of DOX-regulated m^{6}A peaks. In an Integrative Genomics Viewer (IGV) format, normalized m^{6}A-IP and input control coverage are shown in red and gray, respectively. Exons are represented by thick black boxes; 5′ and 3′ untranslated regions (UTRs) are represented by thin black boxes; introns are represented by thin lines. e) GO analysis of transcripts with differentially expressed genes in cells upon DOX treatment.

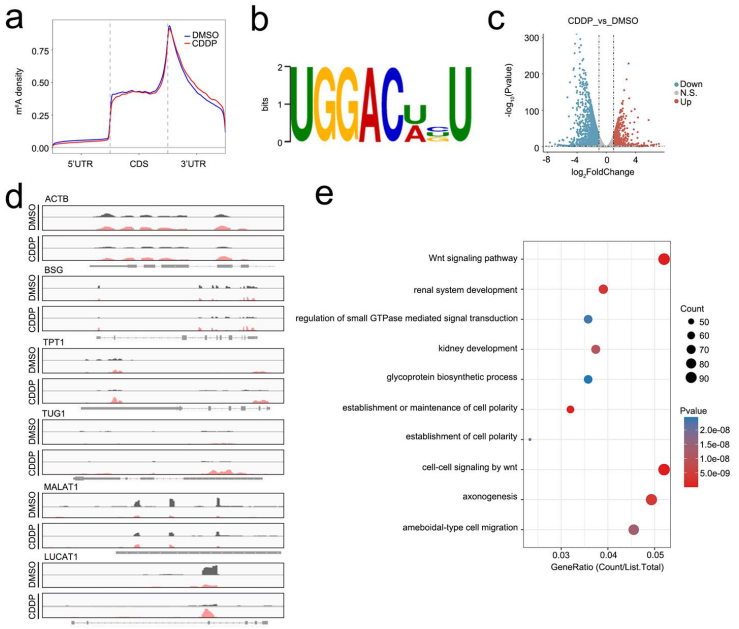

Supplementary Fig. 33 | m^{6}A-Seq profiling of HeLa cells with CDDP treated. a) The normalized distribution of m^{6}A peaks across the start codon, CDS, stop codon of RNAs for DMSO and CDDP treated m^{6}A peaks. b) Sequence logo representing the consensus motif relative to m^{6}A in response to CDDP. c) Volcanic diagram of differentially expressed genes in cells upon CDDP treatment. d) Examples of CDDP-regulated m^{6}A peaks. In an Integrative Genomics Viewer (IGV) format, normalized m^{6}A-IP and input control coverage are shown in red and gray, respectively. Exons are represented by thick black boxes; 5′ and 3′ untranslated regions (UTRs) are represented by thin black boxes; introns are represented by thin lines. e) GO analysis of transcripts with differentially expressed genes in cells upon CDDP treatment.

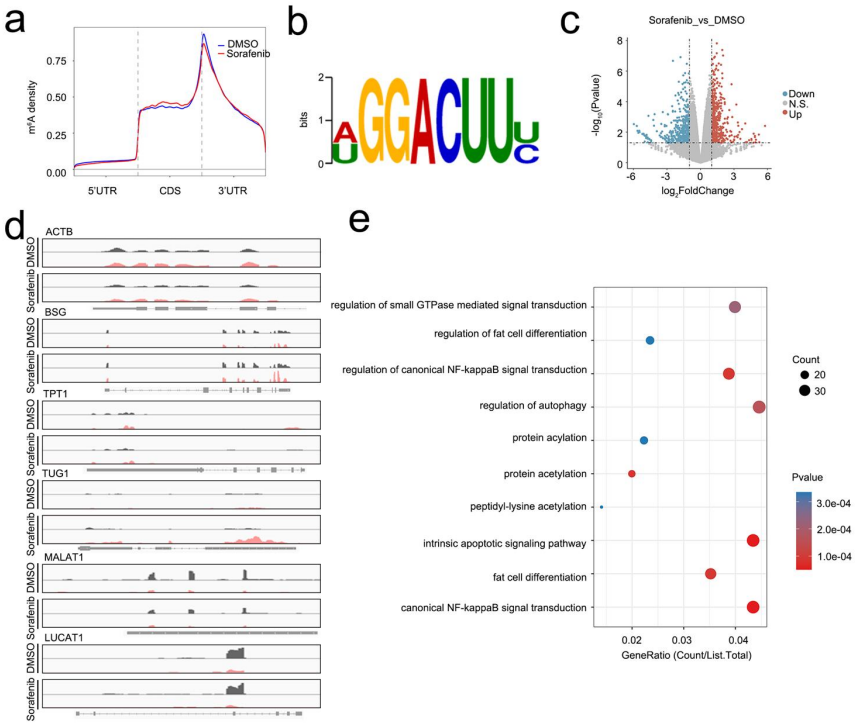

Supplementary Fig. 34 | m^{6}A-Seq profiling of HeLa cells with Sorafenib treated. a) The normalized distribution of m^{6}A peaks across the start codon, CDS, stop codon of RNAs for DMSO and Sorafenib treated m^{6}A peaks. b) Sequence logo representing the consensus motif relative to m^{6}A in response to Sorafenib. c) Volcanic diagram of differentially expressed genes in cells upon Sorafenib treatment. d) Examples of Sorafenib-regulated m^{6}A peaks. In an Integrative Genomics Viewer (IGV) format, normalized m^{6}A-IP and input control coverage are shown in red and gray, respectively. Exons are represented by thick black boxes; 5′ and 3′ untranslated regions (UTRs) are represented by thin black boxes; introns are represented by thin lines. e) GO analysis of transcripts with differentially expressed genes in cells upon Sorafenib treatment.

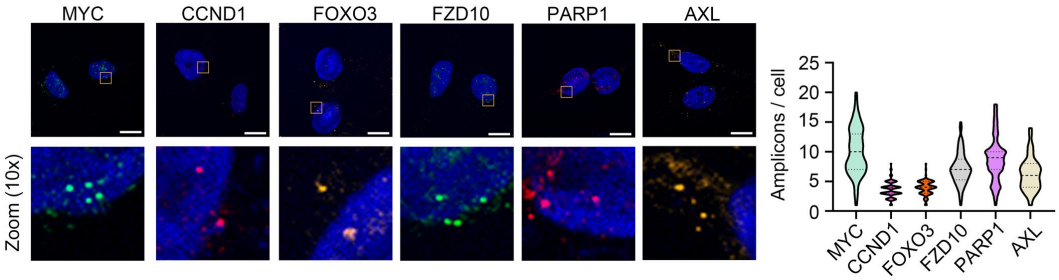

Supplementary Fig. 35 | Fluorescence images of MYC, CCND1, FOXO3, FZD10, PARP1, and AXL mRNA m^{6}A in single cells visualized by PREEM. Scale bars: 10 μm. Right, violin chart of six m^{6}A amplicons counted in single cells (N = 100). N represents the number of single cells for each sample. Source data are provided as a Source Data file.

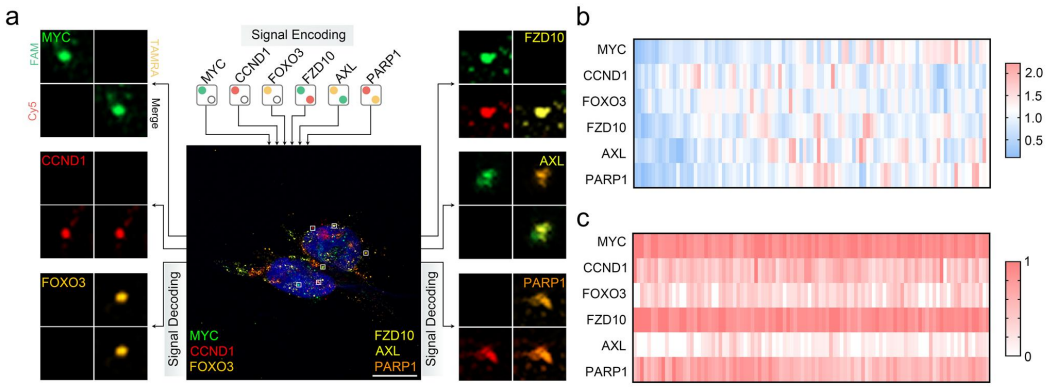

Supplementary Fig. 36 | PREEM for six other m^{6}A RNAs imaging. a) Fluorescence images for the spatial distribution of six other m^{6}A RNAs in HeLa cells. Scale bars: 10 μm. b) Heat map showing expression pattern of six other m^{6}A RNAs by analyzing the amplicons in cells by PREEM. c) Heat map showing subcellular distribution of six other m^{6}A RNAs. All fluorescence measurements were normalized against expression level of the respective marker. Source data are provided as a Source Data file.

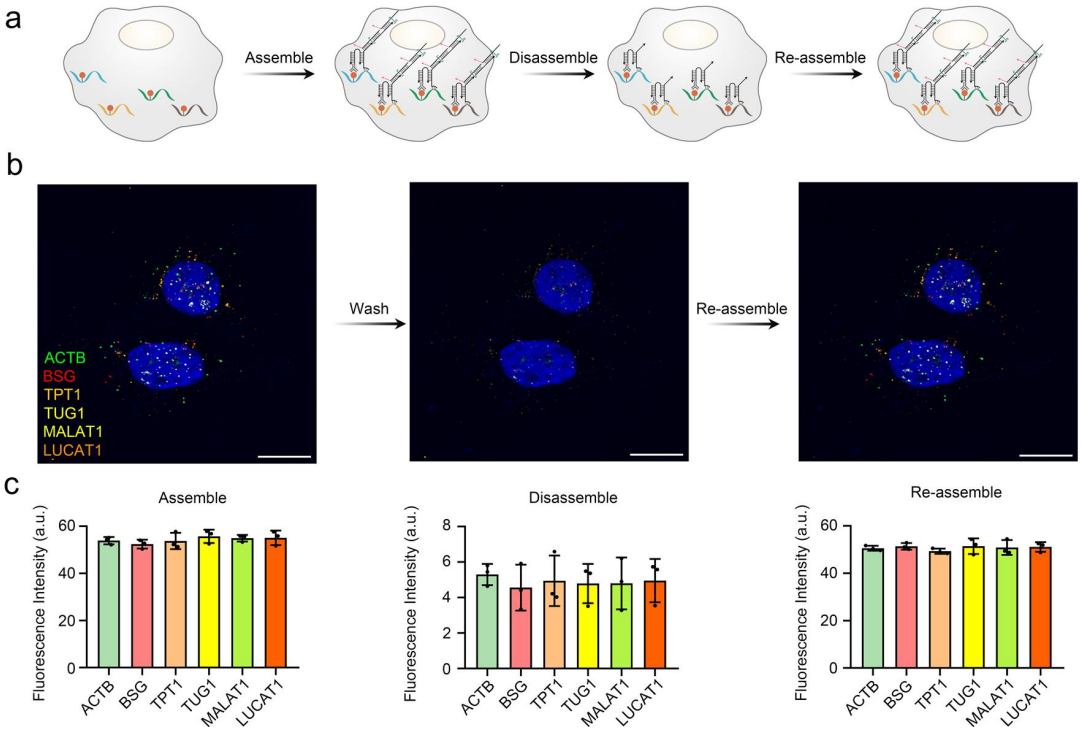

Supplementary Fig. 37 | Cyclic staining and destaining *via* PREEM with reversible HCR. a) Schematic illustration of Cyclic staining and destaining *via* PREEM with reversible HCR. b) Fluorescence images of six m^{6}A RNAs in HeLa cells with staining and destaining cycles from 3 independent experiments. Scale bars: 10 μm. c) Statistical results of fluorescence intensity from the images in Fig. S37b from 3 independent experiments. Data are presented as mean values ± s.d. Error bars represent the standard deviation of three independent experiments. Source data are provided as a Source Data file.

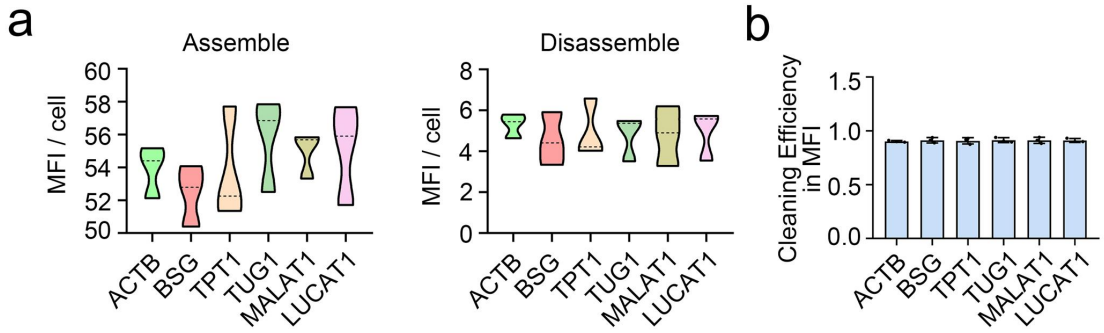

Supplementary Fig. 38 | Quantification of the cleaning efficiency after adding orthogonal washers. a) Violin chart of fluorescence intensity of six m^6A amplicons in single cells in Assemble and Disassemble groups. b) Statistical results of the cleaning efficiency in MFI from the images in Fig. S37a from 3 independent experiments. Data are presented as mean values ± s.d. Error bars represent the standard deviation of three independent experiments. Source data are provided as a Source Data file.

Supplementary tables

Supplementary Table 1 | Sequences of oligonucleotides.

Oligonucleotide sequences used for *in vitro* MMB characterization

Strand	Sequences (5'-3')
Biotin-Target	Biotin-AGCAAGCAGGAGUAUGACGAGUCCGGCCCCUCCAUCGUCCACCGCAAAUGCUUCUAGGCGGm6ACUAUGACUUAGUUGCGUU
DBCO-PH1	DBCO-AA CTTCAGGCGTGCTATT GCCTTGGGTAAGAC ATGGGATTCGATCC GA TA GTCTTACCCAAGGC AATAGCACGCCTGAAG
ID-PH2	TGCGGTGGACGATGGAGGGGCC AA TGGATCT CTTCAGGCGTGCTA TT GCCTTGGGTAAGACTA TC AATAGCACGCCTGAAG AGATCCA
ID-PH2-mod	TGCGGTGGACGATGGAGGGGCC AA-BHQ1-TGGATCT CTTCAGGCGTGCTATT GCCTTGGGTAAGACTA TC AATAGCACGCCTGAAG AGATCCA-FAM
PI	GGATCGAATCCCAT GTCTTACCCAAGGC AATAGCACGCCTGAAG
H1	TGGATCT CTTCAGGCGTGCTATT ATTGGAG AATAGCACGCCTGAAG
H2-FAM	AATAGCACGCCTGAAG AGATCCA CTTCAGGCGTGCTATT CTCCAAT-FAM
Biotin-BSG	Biotin-GGGCCACGGGUCUGUGUUCGACUCAGCCUCAGGGACGACUCUGACCUCUUGGCCm6ACAGAGGACUCACUUGCCCACACCGA
Biotin-TPT1	Biotin-UAUUUUGGAUCUAUCACCUGUCAUCAUAACUGGCUUCUGCUUGUCAUCCm6ACACAACACCAGGACUUAAGACAAAUGGGAC

Oligonucleotide sequences used for *in vitro* PAGE characterization

Strand	Sequences (5'-3')
ACTB-T	AATAGCACGCCTGAAG AGATCCA
ACTB-H1	TGGATCT CTTCAGGCGTGCTATT ATTGGAG AATAGCACGCCTGAAG
ACTB-H2	AATAGCACGCCTGAAG AGATCCA CTTCAGGCGTGCTATT CTCCAAT
BSG-T	AATAGCACGCCTGAAG TGCAACT
BSG-H1	AGTTGCA CTTCAGGCGTGCTATT TGCATGA AATAGCACGCCTGAAG
BSG-H2	AATAGCACGCCTGAAG TGCAACT CTTCAGGCGTGCTATT TCATGCA
TPT1-T	AATAGCACGCCTGAAG ACAGCTT
TPT1-H1	AAGCTGT CTTCAGGCGTGCTATT CGATTAG AATAGCACGCCTGAAG
TPT1-H2	AATAGCACGCCTGAAG ACAGCTT CTTCAGGCGTGCTATT CTAATCG
TUG1-T	AATAGCACGCCTGAAG TTACTGG
TUG1-H1	CCAGTAA CTTCAGGCGTGCTATT AGACCAT AATAGCACGCCTGAAG
TUG1-H2	AATAGCACGCCTGAAG TTACTGG CTTCAGGCGTGCTATT ATGGTCT
MALAT1-T	AATAGCACGCCTGAAG AGGATCA
MALAT1-H1	TGATCCT CTTCAGGCGTGCTATT TTGCTAC AATAGCACGCCTGAAG
MALAT1-H2	AATAGCACGCCTGAAG AGGATCA CTTCAGGCGTGCTATT GTAGCAA
LUCAT1-T	AATAGCACGCCTGAAG TCGATCT
LUCAT1-H1	AGATCGA CTTCAGGCGTGCTATT GCTAATC AATAGCACGCCTGAAG
LUCAT1-H2	AATAGCACGCCTGAAG TCGATCT CTTCAGGCGTGCTATT GATTAGC

Oligonucleotide sequences used for *in situ* cell imaging

Strand	Sequences (5'-3')
ACTB-PH2	TGCGGTGGACGATGGAGGGGCC AA TGGATCT CTTCAGGCGTGCTATT GCCTTGGGTAAGACTA TC AATAGCACGCCTGAAG AGATCCA
ACTB(w.o. m^{6}A)-PH2	CCGCGGCGCGCGGCAGGAAGCC AA TGGATCT CTTCAGGCGTGCTATT GCCTTGGGTAAGACTA TC AATAGCACGCCTGAAG AGATCCA
ACTB-H1	TGGATCT CTTCAGGCGTGCTATT ATTGGAG AATAGCACGCCTGAAG
ACTB-H2-FAM	AATAGCACGCCTGAAG AGATCCA CTTCAGGCGTGCTATT CTCCAAT-FAM
BSG-PH2	GGTCAGAGTCGTCCCTGAGGCT AA AGTTGCA CTTCAGGCGTGCTATT GCCTTGGGTAAGACTATC AATAGCACGCCTGAAG TGCAACT
BSG-H1	AGTTGCA CTTCAGGCGTGCTATT TGCATGA AATAGCACGCCTGAAG
BSG-H2-Cy5	AATAGCACGCCTGAAG TGCAACT CTTCAGGCGTGCTATT TCATGCA-Cy5
TPT1-PH2	AGCAGAAGCCAGTTATGATGAC AA AAGCTGT CTTCAGGCGTGCTATT GCCTTGGGTAAGACTATC AATAGCACGCCTGAAG ACAGCTT
TPT1-H1	AAGCTGT CTTCAGGCGTGCTATT CGATTAG AATAGCACGCCTGAAG
TPT1-H2-TAMRA	AATAGCACGCCTGAAG ACAGCTT CTTCAGGCGTGCTATT CTAATCG-TAMRA
TUG1-PH2	CACGGTGGTAAAGGAAGATAGT AA CCAGTAA CTTCAGGCGTGCTATT GCCTTGGGTAAGACTATC AATAGCACGCCTGAAG TTACTGG
TUG1-H1-FAM	CCAGTAA CTTCAGGCGTGCTATT AGACCAT AATAGCACGCCTGAAG-FAM
TUG1-H2-Cy5	AATAGCACGCCTGAAG TTACTGG CTTCAGGCGTGCTATT ATGGTCT-Cy5
MALAT1-PH2	TAAGTTGGTAATTACTCTTGAT AA TGATCCT CTTCAGGCGTGCTATT GCCTTGGGTAAGACTATC AATAGCACGCCTGAAG AGGATCA
MALAT1-H1-FAM	TGATCCT CTTCAGGCGTGCTATT TTGCTAC AATAGCACGCCTGAAG-FAM
MALAT1-H2-TAMRA	AATAGCACGCCTGAAG AGGATCA CTTCAGGCGTGCTATT GTAGCAA-TAMRA
LUCAT1-PH2	AGAAGTCAGAACACATAGTGTG AA AGATCGA CTTCAGGCGTGCTATT GCCTTGGGTAAGACTATC AATAGCACGCCTGAAG TCGATCT
LUCAT1-H1-TAMRA	AGATCGA CTTCAGGCGTGCTATT GCTAATC

	AATAGCACGCCTGAAG-TAMRA
LUCAT1-H2-Cy5	AATAGCACGCCTGAAG TCGATCT CTTCAGGCGTGCTATT GATTAGC-Cy5
CTNNB1-PH2	GTTCTGATTATGTTCAGATAAA AA TGGATCT CTTCAGGCGTGCTATT GCCTTGGGTAAGACTATC AATAGCACGCCTGAAG AGATCCA
MZF1-PH2	CTCTCATGCCACAGGGGCATAG AA TGGATCT CTTCAGGCGTGCTATT GCCTTGGGTAAGACTATC AATAGCACGCCTGAAG AGATCCA
ACTB-probe-Cy3	Cy3-CTCCTTAATGTCACGCACGATTTCCCGCTCCGGACTCGTCA TACTCCTGCTTGCTGATTCATGAGGTAGTCAGTCAGGTCCCG
BSG-probe-Cy3	Cy3-TGGCGGACGTTCTTGCCTTTGTC
TPT1-probe-Cy3	Cy3-CTCACGGTAGTCCAATAGAGCAA
MALAT1-probe-Cy3	Cy3-TGTTATGCCTGGTTAGGTATGAGC
TUG1-probe-Cy3	Cy3-CAAAGTAGAAATCCCACAACCAAC
LUCAT1-probe-Cy3	Cy3-CAAGGTCCCATAAGAGTTCCAG

Oligonucleotide sequences used for reversible PREEM-based cyclic imaging

Strand	Sequences (5'-3')
ACTB-tH1	AACAAGC TGGATCT CTTCAGGCGTGCTATT ATTGGAG AATAGCACGCCTGAAG
ACTB-tw	AAT AGC ACG CCT GAA GAG ATC CAG CTT GTT
BSG-tH1	TACTACG AGTTGCA CTTCAGGCGTGCTATT TGCATGA AATAGCACGCCTGAAG
BSG-tw	AAT AGC ACG CCT GAA GTG CAA CTC GTA GTA
TPT1-tH1	TGACAGA AAGCTGT CTTCAGGCGTGCTATT CGATTAG AATAGCACGCCTGAAG
TPT1-tw	AAT AGC ACG CCT GAA GAC AGC TTT CTG TCA
TUG1-tH1-FAM	ATGGTTG CCAGTAA CTTCAGGCGTGCTATT AGACCAT AATAGCACGCCTGAAG-FAM
TUG1-tw	AAT AGC ACG CCT GAA GTT ACT GGC AAC CAT
MALAT1-tH1-FAM	TTGAGAG TGATCCT CTTCAGGCGTGCTATT TTGCTAC AATAGCACGCCTGAAG-FAM
MALAT1-tw	AAT AGC ACG CCT GAA GAG GAT CAC TCT CAA
LUCAT1-tH1-TAMRA	TATGCTG AGATCGA CTTCAGGCGTGCTATT GCTAATC AATAGCACGCCTGAAG-TAMRA
LUCAT1-tw	AAT AGC ACG CCT GAA GTC GAT CTC AGC ATA
MYC-PH2	CGC AGG GCA AAA AAG CTC CGT T AA AGATGGT CTTCAGGCGTGCTATT GCCTTGGGTAAGACTA TC AATAGCACGCCTGAAG ACC ATC T
MYC-tH1	TCTGCAT AGATGGT CTTCAGGCGTGCTATT TCCAGAA AATAGCACGCCTGAAG
MYC-H2-FAM	AATAGCACGCCTGAAG ACC ATC T CTTCAGGCGTGCTATT TTC

	TGG A-FAM
FOXO3-PH2	TCT AAT TTC TCA TCA AAA AGT A AA TTAGGTG CTTCAGGCGTGCTATT GCCTTGGGTAAGACTA TC AATAGCACGCCTGAAG CAC CTA A
FOXO3-tH1	TGGACAA TTAGGTG CTTCAGGCGTGCTATT ACAAGCT AATAGCACGCCTGAAG
FOXO3-H2-TAMRA	AATAGCACGCCTGAAG CAC CTA A CTTCAGGCGTGCTATT AGC TTG T-TAMRA
CCND1-PH2	AAG AGC AAA GGA AAA AAC AAC C AA AGAGTGA CTTCAGGCGTGCTATT GCCTTGGGTAAGACTA TC AATAGCACGCCTGAAG TCA CTC T
CCND1-tH1	AGCCATT AGAGTGA CTTCAGGCGTGCTATT ATTACGG AATAGCACGCCTGAAG
CCND1-H2-Cy5	AATAGCACGCCTGAAG TCA CTC T CTTCAGGCGTGCTATT CCG TAA T-Cy5
PARP1-PH2	CGC CGA CTC CCC AGA AGG CAC T AA AAGACTG CTTCAGGCGTGCTATT GCCTTGGGTAAGACTA TC AATAGCACGCCTGAAG CAG TCT T
PARP1-tH1-TAMRA	AGCTAGA AAGACTG CTTCAGGCGTGCTATT AGGTGAA AATAGCACGCCTGAAG-TAMRA
PARP1-H2-Cy5	AATAGCACGCCTGAAG CAG TCT T CTTCAGGCGTGCTATT TTC ACC T-Cy5
AXL-PH2	AGT GGC ACG ATC TTG GCT CAC T AA TAATGCC CTTCAGGCGTGCTATT GCCTTGGGTAAGACTA TC AATAGCACGCCTGAAG GGC ATT A
AXL-tH1-FAM	ATGTGTC TAATGCC CTTCAGGCGTGCTATT TGTTCGA AATAGCACGCCTGAAG-FAM
AXL-H2-TAMRA	AATAGCACGCCTGAAG GGC ATT A CTTCAGGCGTGCTATT TCG AAC A-TAMRA
FZD10-PH2	GCT GGC CCC GGC TCT CCA CCC C AA ATGAACG CTTCAGGCGTGCTATT GCCTTGGGTAAGACTA TC AATAGCACGCCTGAAG CGT TCA T
FZD10-tH1-FAM	TAGGTTC ATGAACG CTTCAGGCGTGCTATT AACGATG AATAGCACGCCTGAAG-FAM
FZD10-H2-Cy5	AATAGCACGCCTGAAG CGT TCA T CTTCAGGCGTGCTATT CAT CGT T-Cy5

Oligonucleotide sequences used for gene knock down

Strand	Sequences (5’-3’)
siMETTL3s	GCUACCUGGACGUCAGUAUdTdT
siMETTL3a	AUACUGACGUCCAGGUAGCdTdT
siACTBs	CCAGCCAUGUACGUUGCUAdTdT
siACTBa	UAGCAACGUACAUGGCUGGdTdT

RT-qPCR primer for RNA quantification in Hela cells

Strand	Sequences (5'-3')
18S-F	CAGCCACCCGAGATTGAGCA
18S-R	TAGTAGCGACGGGCGGTGTG
ACTB-F	AGATGTGGATCAGCAAGC
ACTB-R	TCATCTTGTTTTCTGCGC
METTL3-F	GGAATCACCTCCGACACTC
METTL3-R	AAGCTGCACTTCAGACGAAT
BSG-F	CACCTGTGTCGCCCCAATA
BSG-R	TACGGTAGTGAAGACTGTGCC
TPT1-F	GAATCCAGATGGCATGGTTGC
TPT1-R	CCGCCACAAAGACAGACAGAA
TUG1-F	CACTCATCCTGTGCCTCCTG
TUG1-R	TGATGGCTGAATGCCTCCTG
MALAT1-F	CGTAACGGAAGTAATTCAAG
MALAT1-R	GTCAATTAATGCTAGTCCTC
LUCAT1-F	GGATGAGACTTAGCGTGCCT
LUCAT1-R	CCTCGGGTTGCCTCTGTTTA
U6-F	CTCGCTTCGGCAGCACA
U6-R	AACGCTTCACGAATTTGCGT
GAPDH-F	GGATTGTCTGGCAGTAGCC
GAPDH-R	ATTGTGAAAGGCAGGGAG

Supplementary Table 2 | The average copy number of single-cell RNAs profiled by FISH and single-cell m^{6}A RNAs profiled by PREEM.

Gene	PREEM for m^{6}A site (copy number/cell)	FISH (copy number/cell)	Detected m^{6}A occupancy (%)	Reported m^{6}A occupancy (%)	References
ACTB	14.07	59.76	23.54	21±9(1216th)	27
BSG	7.22	106.95	6.75	6(1335th)	
TPT1	12.16	84.1	14.46	15(687th)	
TUG1	6.06	24.14	25.1	22(1114th)	
MALAT1	14.38	19.41	74.09	80±3 (2577th)	
LUCAT1	3.07	17.97	17.08	-	-